# A Role for BLM in Double-Strand Break Repair Pathway Choice: Prevention of CtIP/Mre11-Mediated Alternative Nonhomologous End-Joining

Anastazja Grabarz, Josée Guirouilh-Barbat, Aurélia Barascu, Gaëlle Pennarun, Diane Genet, Emilie Rass, Susanne Germann, Pascale Bertrand, Ian D Hickson, Bernard S. Lopez

Cell Reports
Report



# A Role for BLM in Double-Strand Break Repair Pathway Choice: Prevention of CtIP/Mre11-Mediated Alternative Nonhomologous End-Joining

Anastazja Grabarz,[2,4] Josée Guirouilh-Barbat,[1,2,4] Aurélia Barascu,[1,2] Gaëlle Pennarun,[2] Diane Genet,[2] Emilie Rass,[2] Susanne M. Germann,[3] Pascale Bertrand,[2] Ian D. Hickson,[3] and Bernard S. Lopez[1,2,*]
[1]Université Paris Sud, CNRS UMR 8200, Institut de Cancérologie Gustave-Roussy, 114 Rue Edouard Vaillant, 94805 Villejuif, France
[2]CNRS UMR217, CEA, DSV, Institut de Radiobiologie Cellulaire et Moléculaire, 18 Route du Panorama, Fontenay aux Roses F-92265, France
[3]Nordea Center for Healthy Aging, Department of Cellular and Molecular Medicine, University of Copenhagen, Blegdamsvej 3B, DK-2200 Copenhagen N, Denmark
[4]These authors contributed equally to this work
*Correspondence: bernard.lopez@gustaveroussy.fr
http://dx.doi.org/10.1016/j.celrep.2013.08.034


## SUMMARY

**The choice of the appropriate double-strand break (DSB) repair pathway is essential for the maintenance of genomic stability. Here, we show that the Bloom syndrome gene product, BLM, counteracts CtIP/MRE11-dependent long-range deletions (>200 bp) generated by alternative end-joining (A-EJ). BLM represses A-EJ in an epistatic manner with 53BP1 and RIF1 and is required for ionizing-radiation-induced 53BP1 focus assembly. Conversely, in the absence of 53BP1 or RIF1, BLM promotes formation of A-EJ long deletions, consistent with a role for BLM in DSB end resection. These data highlight a dual role for BLM that influences the DSB repair pathway choice: (1) protection against CtIP/MRE11 long-range deletions associated with A-EJ and (2) promotion of DNA resection. These antagonist roles can be regulated, according to cell-cycle stage, by interacting partners such as 53BP1 and TopIII, to avoid unscheduled resection that might jeopardize genome integrity.**

## INTRODUCTION

DNA double-strand breaks (DSBs) are deleterious lesions leading to genetic rearrangements and cell death. The choice of DSB repair pathway is an essential issue for the balance between genome stability and diversification.

Homologous recombination (HR) and nonhomologous end-joining (NHEJ) are two major mechanisms repairing DSBs. Recently, an alternative end-joining (A-EJ) pathway has been described, which has been proposed to be initiated by single-strand DNA (ssDNA) resection at the DNA ends, driven by MRE11 and CtIP (Guirouilh-Barbat et al., 2004; Bennardo et al., 2008; Rass et al., 2009; Xie et al., 2009; Deriano et al., 2009). While both canonical NHEJ (C-NHEJ) and HR are necessary for genome maintenance, A-EJ is highly error-prone and is a major source of chromosomal translocations (Boboila et al., 2010; Guirouilh-Barbat et al., 2004; Weinstock et al., 2007; Yan et al., 2007).

The RecQ helicase BLM has been also shown to be involved in ssDNA resection at the initial stages of HR (Gravel et al., 2008; Nimonkar et al., 2011). Since ssDNA resection can also lead to A-EJ, this raises the question of whether BLM might play a putative role in A-EJ. Conversely, BLM is required for the localization of 53BP1 at arrested replication forks in an ATR/ATM-dependent manner (Davalos et al., 2004; Tripathi et al., 2007). 53BP1 suppresses CtIP-mediated resection (Bouwman et al., 2010; Bunting et al., 2010), which suggests a protective role for BLM against A-EJ. Consistently, mutations in *BLM* lead to Bloom syndrome (BS), a rare autosomal-recessive genetic disorder associated with high levels of spontaneous sister-chromatid exchanges (SCEs), genome instability, and cancer predisposition (Chu and Hickson, 2009). Thus, two apparently opposite roles could be proposed for BLM at A-EJ initiation.

Here, we analyzed the role of BLM in A-EJ using an intrachromosomal substrate that we previously showed permits the characterization of A-EJ at the molecular level in a chromosomal context (Guirouilh-Barbat et al., 2004, 2007; Rass et al., 2009). Our data highlight a dual role for BLM in the prevention/promotion of DNA end degradation and the importance of the balance between BLM and 53BP1 in preventing deleterious DNA degradation initiated by CtIP/MRE11. We propose that BLM is a pivotal actor at an early step in DSB repair pathway choice.

## RESULTS

### BLM Protects against Large Deletions at A-EJ Junctions

Using the substrate depicted in Figure 1A, we previously characterized the A-EJ pathway, which systematically deletes the four 3′-protruding nucleotides (3′-Pnt) at the junctions. In contrast, C-NHEJ uses at least one of the four 3′-Pnt (Guirouilh-Barbat et al., 2004, 2007; Rass et al., 2009).

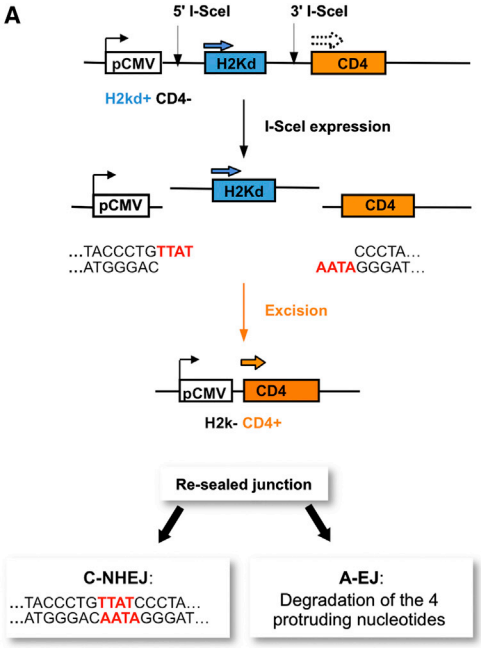


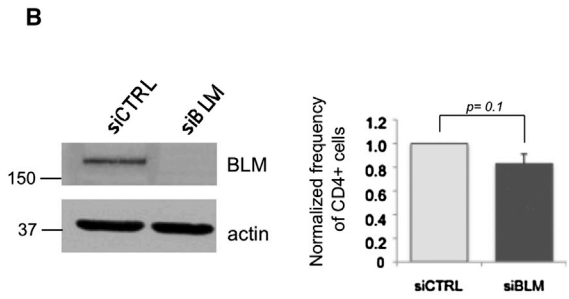


| | siCTRL | siBLM |
|---|---|---|
| Use of 3'-Pnt (C-NHEJ) | **50.5%** | **40.7%** |
| Del of 3' Pnt (A-EJ) | **49.5%** | **59.3%** |
| Nb of sequences | 91 | 54 |

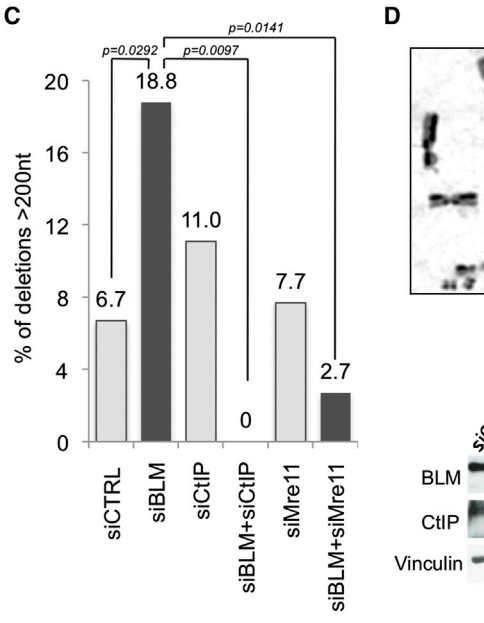


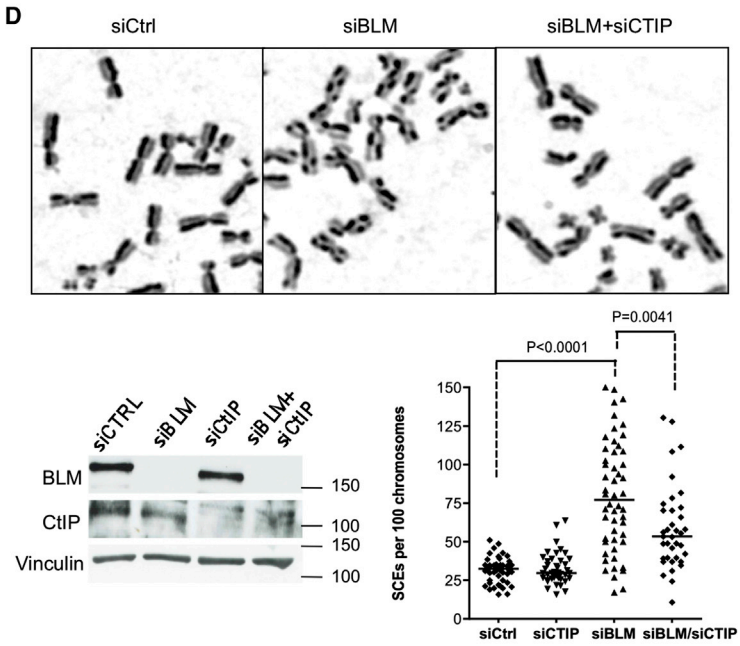


| | siCtrl | siCTIP | siBLM | siBLM/siCTIP |
|---|---|---|---|---|
| SCEs/100 chromosomes (mean±SE) | 31.6±1.1 | 32.6±1.6 | 79.5±5.0 | 58.8±4.5 |
| Number of metaphases | 50 | 40 | 52 | 37 |
| Chromosomes scored | 2304 | 1746 | 2244 | 1674 |

**Figure 1. BLM Protects against CtIP/MRE11-Dependent Long-Range Deletions and SCEs**

(A) The intrachromosomal end-joining substrate. In the absence of expression of the meganuclease I-SceI, *CD4* is not expressed as it is too far from the promoter. Two I-SceI cleavage sites flank the fragment containing *H2Kd*. After cleavage by I-SceI, rejoining of the DNA ends leads to the excision of the internal H2Kd fragment and the expression of *CD4*. These events were measured by fluorescence-activated cell sorting (FACS) and the resealed junctions were amplified by PCR and sequenced.

(B) BLM silencing in GC92 cells. Upper panel: expression of BLM. Histograms show efficiency of total end-joining. The values correspond to five independent experiments (p = 0.1). The error bars correspond to SEM. Lower panel: frequencies of C-NHEJ versus A-EJ.

(C) Percentage of long-range deletions (>200 bp) upon BLM silencing in combination with silencing of either CtIP or MRE11.

*(legend continued on next page)*

Silencing of BLM in wild-type (WT) fibroblasts did not significantly decrease the global end-joining efficiency (Figure 1B). However, sequence analysis of the repair junctions revealed an alteration of the repair pattern upon BLM silencing: a small decrease in the frequency of 3′-Pnt use, accompanied by a slight increase in the frequency of the 3′-Pnt deletion events (Figures 1B and S1). Importantly, the silencing of BLM significantly affected the distribution of deletion sizes among deletion end-joining events (Figure S1 and Table S1). Indeed, the frequency of large deletions (>200 bp) was 2.8-fold increased (Figure 1C, Figure S1, and Table S1), showing that BLM protects against extended deletions generated by A-EJ.

## BLM Protects against CtIP/MRE11-Dependent Long-Range Deletions and SCEs

It has been proposed that A-EJ-associated deletions result from ssDNA resection of DSB ends (Rass et al., 2009). Strikingly, depletion of CtIP in the BLM-silenced cells totally abolished the long deletions events normally seen in BLM-depleted cells (Figure 1C). Moreover, silencing MRE11 also strongly decreased long-range deletions generated by loss of BLM (Figure 1C), consistent with the fact that CtIP acts as a cofactor of MRE11 for resection (Eid et al., 2010; Sartori et al., 2007). These data reveal an additional role for BLM in genome stability maintenance: protection against CtIP/MRE11-mediated long-range deletions promoted by A-EJ.

A hallmark of BS cells is their high level of spontaneous SCEs. Accordingly, silencing BLM in the WT fibroblast used here significantly increased the level of SCEs. Strikingly, whereas silencing CtIP did not affect the frequency of SCEs in the control cells, it partly rescued the frequency of SCEs in BLM-depleted cells (Figure 1D). Thus, CtIP is responsible in part for the high level of spontaneous SCEs in the absence of BLM, and hence BLM protects against CtIP-induced SCEs.

## 53BP1, RIF1, and BLM Act in an Epistatic Manner for Protection against A-EJ Long-Range Deletions

We next aimed at obtaining insights into the molecular mechanism by which BLM represses CtIP-mediated A-EJ. The 53BP1 protein was a promising candidate, because it counteracts resection during HR initiation and class switch recombination (Bunting et al., 2010; Bothmer et al., 2010) and interacts with BLM upon replication stress (Sengupta et al., 2004; Tripathi et al., 2008).

Hence, we depleted 53BP1 in order to study its role in A-EJ (Figure 2A). The sequence of the repair junctions showed that silencing 53BP1 slightly reduced the frequency of 3′-Pnt use (Figure 2B). More importantly, the distribution of the deletion sizes was also significantly affected by silencing 53BP1 (Figure 2C, Figure S2, and Table S2): the frequency of long deletions (>200 bp) increased more than 4-fold upon silencing of 53BP1. Silencing CtIP in 53BP1-depleted cells rescued both the frequency of 3′-Pnt use and the frequency of long deletions generated by 53BP1 silencing (Figures 2B and 2C, Figure S2, and Table S2). Interestingly, simultaneous silencing of both BLM and 53BP1 decreased the frequency of 3′-Pnt use to the level seen with 53BP1 silencing alone (Figures 2B and Table S2) but did not further increase the frequency of long-size deletions (Figure 2C, Figure S2, and Table S2).

RIF1, which is a partner of 53BP1 for protection against resection (Chapman et al., 2013; Di Virgilio et al., 2013; Escribano-Díaz et al., 2013), is required for BLM focus formation (Feng et al., 2013). Remarkably, silencing RIF1 increased the frequency of long-range deletions in an epistatic way with 53BP1. Moreover, simultaneous silencing of both BLM and RIF1 did not further increase the frequency of long-range deletions (Figure 2D, Figure S2, and Table S2). These data show that BLM, 53BP1, and RIF1 act in an epistatic manner for protection against A-EJ large deletions.

Surprisingly, while BLM protects against A-EJ long-range deletions in WT cells, silencing BLM in cells depleted of 53BP1 or RIF1 decreased the frequency of such events close to the frequency in cells silenced for BLM alone (Figures 2C and 2D). This suggests that BLM is involved in generating some of the deletion events found in 53BP1- or RIF1-depleted cells. These data reveal two opposite roles for BLM: (1) protection against CtIP-mediated long-range deletions, in association with 53BP1 and RIF1, and (2) the promotion of long-range deletions, when 53BP1 or RIF1 are absent. This second role is consistent with an involvement of BLM in DNA end resection.

## BLM Favors the Assembly of Both Radiation-Induced 53BP1 and pRPA Foci

We then addressed the question of the colocalization of BLM and 53BP1 after ionizing radiation (IR), which efficiently generates DSBs. Confocal analysis revealed that most of the BLM foci colocalized with 53BP1 foci after IR (Figure 3A). Using the proximity ligation assay (PLA), a fluorescent signal requiring the presence of both BLM and 53BP1 was detected, showing their close localization in situ (Figures 3B and S3A). Moreover, coimmunoprecipitation of endogenous BLM and 53BP1 proteins was stimulated by IR. Interestingly, this interaction was abolished by treatment with an ATM inhibitor (Figure S3B).

Using an antibody specific for BLM phosphorylated on Thr99 (pT99BLM), which is the residue phosphorylated by ATM, we show that pT99BLM interacted in situ with 53BP1 after IR (Figure 3B). Moreover, pT99BLM and 53BP1 interacted in all cell-cycle phases, but with a slight reduction in the S and G2 phases compared to the G1/S phase (Figure 3C). In contrast, PLA analysis showed an increase (more than 2-fold) of the IR-induced interaction of pT99BLM with its canonical partner TopIII$\alpha$ in S and G2 phases (Figure 3C). Interestingly, IR stimulated the in situ colocalization of 53BP1 and TopIII$\alpha$ in S and G2 phases (Figure 3C). These data show that the

(D) Impact of CtIP silencing on SCEs induced by BLM depletion in GC92 cells. Upper panel: examples of SCEs. Middle panel: expression of BLM and CtIP (left) and quantification of SCEs (right). The horizontal lines on the scatterplot indicate the median. Lower panel: number of metaphases and chromosomes counted in each condition.

See also junction sequences in Table S1 and deletion distribution in Figure S1.

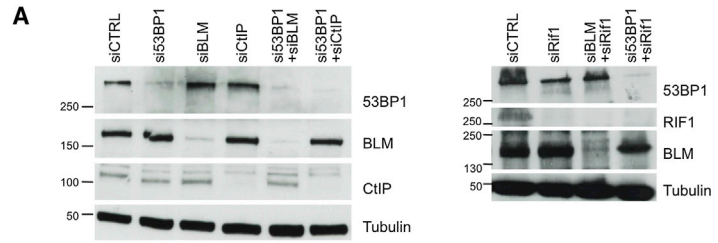


B

| | siCTRL | si53BP1 | siCtIP | si53BP1 +siCtIP | siBLM | si53BP1 +siBLM | siRIF1 | siBLM +siRIF1 | si53BP1 +siRIF1 |
|---|---|---|---|---|---|---|---|---|---|
| Use of 3'-Pnt (C-NHEJ) | **50.5%** | **33.3%** | 52.0% | **46.0%** | **40.7%** | **30.2%** | **44.2%** | **41.7%** | **39.5%** |
| Del of 3' Pnt (A-EJ) | **49.5%** | **66.7%** | 48.0% | **54.0%** | **59.3%** | **69.8%** | **55.8%** | **58.3%** | **60.5%** |
| Nb of sequences | 91 | 42 | 75 | 50 | 54 | 53 | 43 | 48 | 43 |

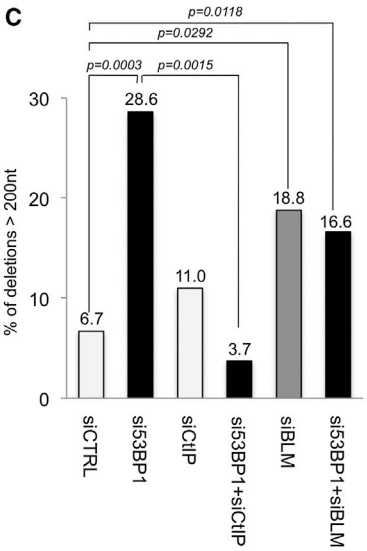


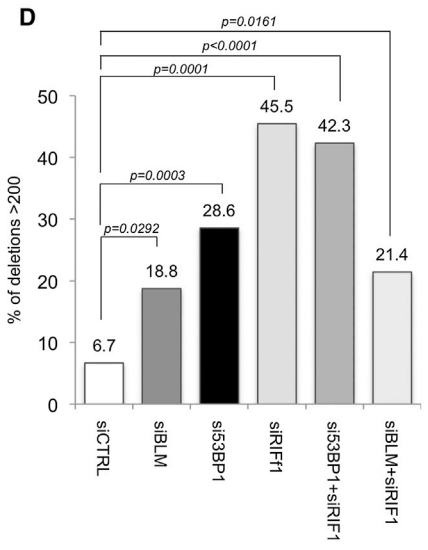


**Figure 2. 53BP1, RIF1, and BLM Act in an Epistatic Manner for Protection against A-EJ Long-Range Deletions**

(A) Silencing of 53BP1, BLM, RIF1 or CtIP in GC92 cells.

(B) Frequencies of C-NHEJ versus A-EJ events.

(C) Percentage of long-range deletions (>200 bp) upon 53BP1, BLM, or CtIP silencing.

(D) Percentage of long-range deletions (>200 bp) upon RIF1, 53BP1, or BLM silencing.

See junction sequences in Table S2 and deletion distribution in Figure S2.

BLM/53BP1 interaction is favored in the G1 phase, while the assembly of the complex with TopIII$\alpha$ occurs in the S and G2 phases. The G1 phase is generally considered not to be permissive for HR, which is initiated by DSB end resection, while the S and G2 phases are. These data are thus consistent with the fact that TopIII$\alpha$ enhances BLM helicase activity, which is required for its role in resection.

Next, we addressed the impact of BLM on IR-induced 53BP1 foci by undertaking a comparison of a BS cell line (PSNG13) with counterparts complemented with either a WT *BLM* cDNA (PSNF5) or one encoding a BLM protein mutated on residue Thr99 (cell line PSN T99A), which is not able to be phosphorylated by ATM. Notably, this mutation abolishes the interaction with 53BP1 after replication stress and fails to correct radiosensitivity and chromosomal aberrations in BS cells (Beamish et al., 2002; Davies et al., 2004; Goodarzi and Lees-Miller, 2004; Tripathi et al., 2008). While BS cells were very inefficient in the assembly of 53BP1 foci, complementation with WT BLM restored efficient 53BP1 foci formation after IR (Figure 4A). Interestingly, the ATM phosphorylation mutant failed to efficiently rescue IR-induced 53BP1 foci (Figure 4A). These data show that BLM favors the assembly of 53BP1 foci after IR in a process requiring its phosphorylation on Thr99.

The above data raised an apparent contradiction. On one hand, BLM is necessary for the recruitment of 53BP1 at DSBs, where 53BP1 protects against resection, while on the other, BLM has been shown to promote ssDNA resection in in vitro experiments or upon exposure to camptothecin (Gravel et al., 2008; Nimonkar et al., 2011). In mammalian cells, resection is frequently analyzed by monitoring phospo-RPA (pRPA) foci that label ssDNA. Here, we show the involvement of BLM in the assembly of pRPA foci after IR (Figure 4B). Importantly, complementation of BS cells with T99A-BLM failed to restore IR-induced pRPA foci. These data suggest a role for BLM in resection at IR-induced DSBs, which requires its phosphorylation at Thr99. These data are in agreement with the aforementioned association of pT99BLM with TopIII$\alpha$ in the S and G2 cell-cycle phases.

## DISCUSSION

The data presented here reveal a role for BLM in genome stability maintenance at an early step of DSB repair pathway choice: the repression of A-EJ associated with long-range deletions. Indeed, A-EJ is an error-prone pathway both at the repair junction and at the chromosome scale (Boboila et al., 2010; Guirouilh-Barbat et al., 2004; Simsek and Jasin, 2010; Weinstock et al., 2007; Yan et al., 2007). In line with this, in vitro studies monitoring plasmid ligation in BS cell crude extracts (Gaymes et al., 2002), or ligation of episomic plasmids upon BLM ablation, showed a decrease in the fidelity of end-joining, consistent with our data in a chromosomal context. Moreover, it has recently been shown that in *Drosophila*, the absence of BLM leads to increased chromosomal instability linked to A-EJ (Garcia et al., 2011).

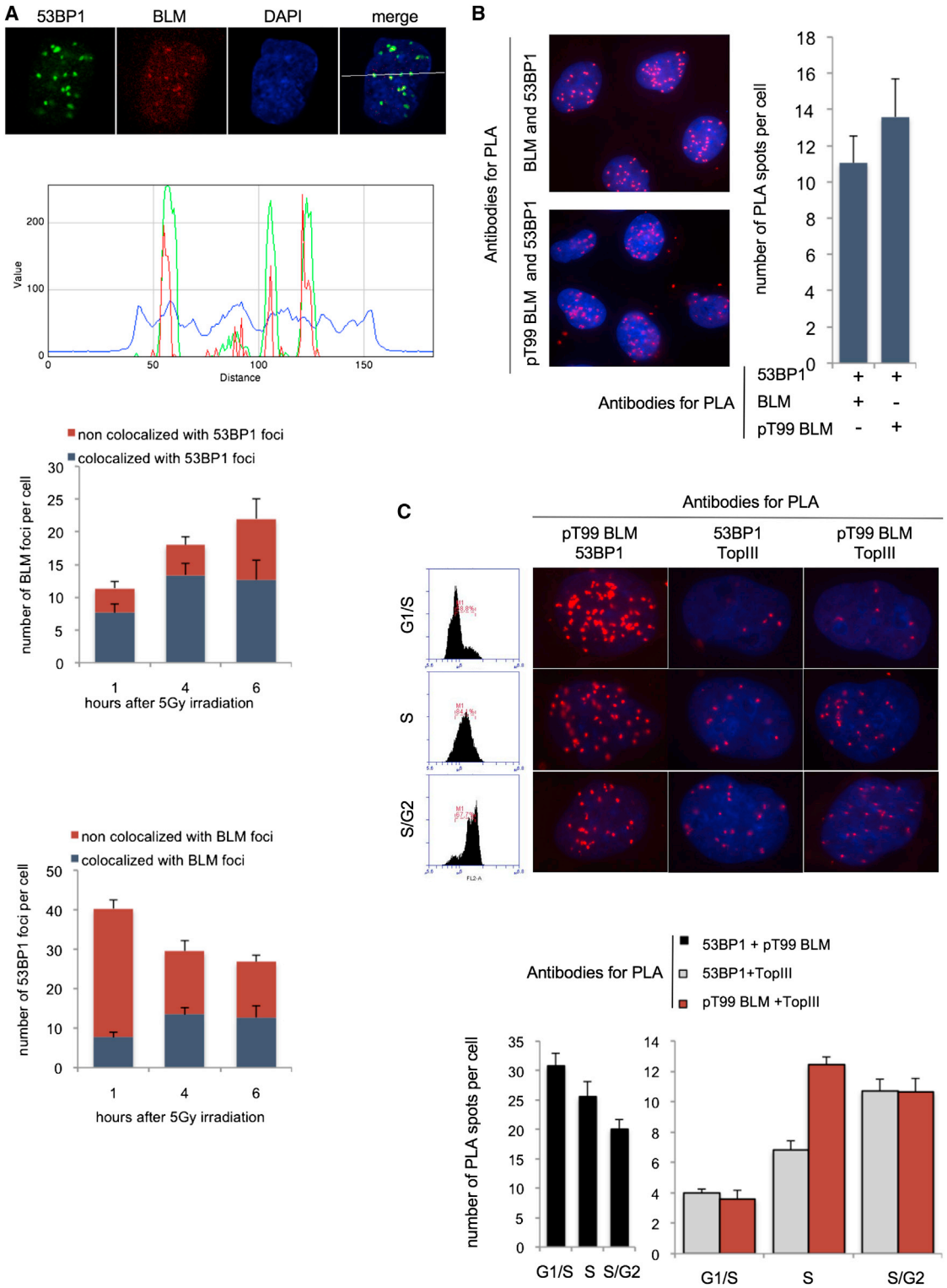


**Figure 3. BLM's Association with 53BP1 and TopoIIIα Is Regulated by the Cell-Cycle Phase**

(A) Confocal analysis of BLM (red) and 53BP1 foci (green) colocalization in irradiated GC92 cells (5 Gy). Upper panel: representative pictures. Middle panel: fluorescence quantification corresponding to the path indicated in the upper panel (merge). Note the correspondence of the peaks of BLM and 53BP1 fluorescence. Bottom panel: quantification of the colocalization of BLM/53BP1 foci (mean ± SEM).

*(legend continued on next page)*

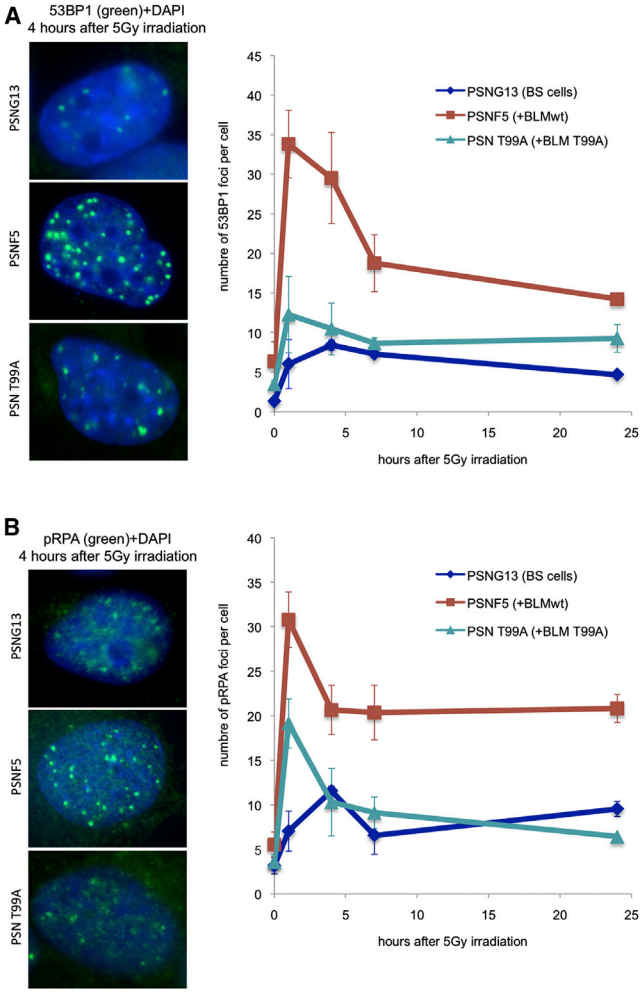


**Figure 4. BLM Favors the Assembly of Both Radiation-Induced 53BP1 and pRPA Foci**

(A) Impact of BLM on 53BP1 focus assembly. Left panel: examples of ionizing radiation (IR)-induced 53BP1 foci (5Gy) in BS cells or in BS cells complemented with BLMwt or BLMT99A. Right panel: quantification (mean ± SEM).

(B) Impact of BLM on pRPA focus assembly. Left panel: examples of IR-induced pRPA foci (5Gy) in BS cells or in BS cells complemented with BLMwt or BLMT99A. Right panel: quantification (mean ± SEM).

BLM plays several roles in HR: the dissolution of Holliday junctions and of abortive HR intermediates, and the promotion of resection to facilitate initiation of HR. The two former roles are antirecombination functions, accounting for the high level of SCEs of BS cells. In contrast, the latter role is a prorecombination function. This raises a paradox, because cells devoid of BLM are not HR defective, but instead exhibit hyperrecombination phenotypes. The data presented here help to resolve this paradox, since they reveal a dual role for BLM: (1) protection against CtIP/MRE11 degradation, which might constitute an additional antirecombination role and which, at least in part, accounts for increased SCEs in BS cells; and (2) the promotion of resection.

It is clear that resection is a double-edged sword. First, it initiates HR, which is essential for maintenance of genome stability; however, excessive initiation of HR can lead to an accumulation of toxic HR intermediates and promote genome rearrangements between repeat sequences. Second, resection also initiates A-EJ events, which are error-prone and can generate profound chromosome rearrangements. Hence, resection should be tightly controlled to secure genome stability. Cell-cycle position is clearly an important issue, since HR is only active in the S and G2 phases, while C-NHEJ and A-EJ are active throughout the cell cycle (for review, see Grabarz et al., 2012). Thus, to avoid A-EJ, resection should be repressed in the G1 phase, when HR is inefficient, but should be permitted in the S and G2 phases, to promote HR. The interaction of BLM and 53BP1 in the G1 phase shown here is consistent with this protective role against A-EJ. The interaction with TopIII$\alpha$ might then favor resection, and hence permit HR initiation in the S and G2 phases. Indeed, the helicase activity of BLM is involved in resection (Nimonkar et al., 2011) and the interaction of TopIII$\alpha$ with BLM enhances its helicase activity. Of note, phosphorylation at Thr99 is required for both of the antagonist roles of BLM, and therefore the balance between the suppression and promotion of resection is likely to be strongly influenced by the binding of protein partners to BLM.

Taken together, our data support a model for DSB repair in which BLM plays a dual role at DSB repair initiation. First, the prevention of A-EJ and long-range CtIP/MRE11-dependent deletions, through interaction with 53BP1. In return, 53BP1 and RIF1 restrain the intrinsic resection activity of BLM. This role should be particularly important in the G1 phase when HR is inactive (2)- initiation of HR via resection, which should be restricted to the S and G2 phases. These two antagonistic roles of BLM can be regulated by interaction with its partners, which can modify BLM's activities according to the position of the cell in the cell cycle. Therefore, BLM is an essential actor in the early stages of DSB repair pathway choice, which must be tightly controlled to ensure the maintenance of genome stability.

## EXPERIMENTAL PROCEDURES

### DNA Manipulations

All DNA manipulations were performed as previously described previously (Ausubel et al., 1999).

### Cells and Transfections

The GC92 cell line (Rass et al., 2009) was derived from SV40-transformed GM639 human WT fibroblasts and contains the end-joining substrate pCOH-CD4 (Guirouilh-Barbat et al., 2004). The PSNG13 cell line is a human

(B) In situ interactions between BLM or pT99 BLM with 53BP1 monitored by PLA. Left panels: representative pictures. Right panel: quantification of BLM/53BP1 or pT99 BLM/53BP1 PLA dots (mean ± SEM). See negative controls in Figure S3A.

(C) In situ interactions according cell cycle. Cells were arrested in G1/S with mimosine and in S/G2 with RO3306. Cell-cycle distributions were analyzed by FACS following mimosine or RO3306 treatment or 7 hr after release from a mimosine arrest (upper left panels). Upper right panel: representative pictures. Bottom panel: quantification of 53BP1/pT99 BLM PLA (left) and pT99 BLM/TopIII and 53BP1/TopIII$\alpha$ PLA (right) in the different cell-cycle phases (mean ± SEM).

SV40-transformed BS fibroblast. PSNF5 is the PSNG13 complemented with the wtBLM, and PSN T99A is the PSNG13 complemented with BLM mutated on the Thr99.

GC92 cells were cultured in Dulbecco's modified Eagle's medium supplemented with 10% fetal calf serum (FCS), 2 mM glutamine, and 200 IU/ml penicillin and incubated at 37°C in 5% $CO_2$. PSNG13, PSNF5, and PSN T99A were cultured in minimum essential medium alpha medium supplemented with 10% FCS and 350 μg/ml neomycin and incubated at 37°C in 5% $CO_2$.

I-SceI was expressed by the transient transfection of the cells with the expression plasmid pCMV-I-SceI (Liang et al., 1998). The expression of the hemagglutinin (HA)-tagged I-SceI was verified by western blotting or immunofluorescence using an anti-HA antibody (MMS-101R, Covance).

The small interfering RNA (siRNA) sequences were as follows: siBLM, 5′-UUAAUUUACAGAUGUGCUCUU-3′; si53BP1 (Dharmacon "Smart pool"), siCtIP, 5′-GCUAAAACAGGAACGAAUC-3′; siMRE11, 5′-GAUGCCAUUGAG GAAUAAG-3′; and siRIF1: 5′- GCUCUAUUGUUAGGUCCCAUUCU-3′. The siRNA complexes were incubated with the cells for 48 hr and removed prior to I-SceI transfection, as described above.

IR was performed using a $^{137}$Cs source (2 Gy/min).

### Cell Synchronization

Cells were incubated for 20 hr before analysis with Mimosin (250 μM [Sigma], for G1/S arrest) or the inhibitor of Cdk1 RO3306 (5 μM [Calbiochel], for G2 arrest). For cells in S phase, mimosin was added to the medium overnight and cells were analyzed 7 hr after the drug release.

### Western Blotting

Protein extracts (25–50 μg) were resolved using 8% SDS-PAGE, transferred to a nitrocellulose membrane, and probed with the following specific antibodies: anti-BLM (Abcam #Ab2179), anti-CtIP (rabbit, courtesy of Dr. R. Baer), anti-53BP1 (Cell Signaling Technology #4937), anti-RIF1 (Bethyl Laboratories, #A300-569), anti-vinculin (Abcam #Ab18058), and anti-actin or anti-tubulin (Sigma #A2066 and #T5168, respectively). Immunoreactivity was visualized using an enhanced chemiluminescence detection kit (EZ-ECL, Biological Industries).

### Immunofluorescence and PLA Assays

The cells were seeded onto slides, treated and fixed in 2% PFA for 20 min, washed in PBS, and permeabilized by ice-cold 70% ethanol (overnight) or by 10 min in PBS, Triton 0.5%. The slides were then saturated with PBS, Tween 0.05%, and BSA 2% and probed with the following antibodies: anti-BLM, anti-53BP1 (see above), anti-BLM (Becton Dickinson #612522), anti-Topoisomerase III (Abcam #Ab49673), and pT99BLM (rabbit, courtesy of Dr. Y. Pommier). Foci colocalization was analyzed with Image J. The PLA assays (Olink Bioscience) were conducted using the manufacturer's protocol with antibody staining as performed in the standard immunofluorescence procedure.

### Junction Sequence Analysis

Junction analyses were performed as previously described (Guirouilh-Barbat et al., 2004; Rass et al., 2009).

### SCE Assay

The SCE assay was performed according to the standard fluorescence-plus-Giemsa procedure (Perry and Wolff, 1974), with some modifications. The cells (GC92) were plated 24 hr prior to siRNA transfection. Twenty-four hours after transfection, 10 μM BrdU (Sigma) was added to the medium and the cells were grown for a further 48 hr. Colchicine (Sigma) was added during the final 2 hr to a final concentration of 0.1 μg/ml. Metaphase spreads were captured using bright-field microscopy (Leica DM5500) with a 100× objective lens (HCX PL APO, Leica).

### Statistical Analysis

Statistical analyses (Mann-Whitney tests) were performed using GraphPad Prism 3.0 (GraphPad Software).

## SUPPLEMENTAL INFORMATION

Supplemental Information includes three figures and two tables and can be found with this article online at http://dx.doi.org/10.1016/j.celrep.2013.08.034.

## ACKNOWLEDGMENTS

We thank Dr. M. Jasin for the *I-SceI* expression plasmids and Elodie Dardillac and Caroline Chabance for helpful technical assistance. B.S.L. was supported by ANR (National Agency for Research), Association for Research against Cancer (Fondation ARC), and the Institut National du Cancer; P.B. was supported by Fondation ARC and Ligue contre le Cancer-comité Ile de France; I.H. was supported by the Nordea Foundation (Denmark) and the Danish Medical Research Council (FSS); and A.G. was supported by a fellowship from ARC.

Received: February 26, 2013
Revised: July 25, 2013
Accepted: August 21, 2013
Published: October 3, 2013

## REFERENCES

Ausubel, F.M., Brent, R., Kingston, R.E., Moore, D.D., Seidman, J.G., Smith, J.A., and Struhl, K. (1999). Current Protocols in Molecular Biology (Boston: John Wiley & Sons).

Beamish, H., Kedar, P., Kaneko, H., Chen, P., Fukao, T., Peng, C., Beresten, S., Gueven, N., Purdie, D., Lees-Miller, S., et al. (2002). Functional link between BLM defective in Bloom's syndrome and the ataxia-telangiectasia-mutated protein, ATM. J. Biol. Chem. *277*, 30515–30523.

Bennardo, N., Cheng, A., Huang, N., and Stark, J.M. (2008). Alternative-NHEJ is a mechanistically distinct pathway of mammalian chromosome break repair. PLoS Genet. *4*, e1000110.

Boboila, C., Jankovic, M., Yan, C.T., Wang, J.H., Wesemann, D.R., Zhang, T., Fazeli, A., Feldman, L., Nussenzweig, A., Nussenzweig, M., and Alt, F.W. (2010). Alternative end-joining catalyzes robust IgH locus deletions and translocations in the combined absence of ligase 4 and Ku70. Proc. Natl. Acad. Sci. USA *107*, 3034–3039.

Bothmer, A., Robbiani, D.F., Feldhahn, N., Gazumyan, A., Nussenzweig, A., and Nussenzweig, M.C. (2010). 53BP1 regulates DNA resection and the choice between classical and alternative end joining during class switch recombination. J. Exp. Med. *207*, 855–865.

Bouwman, P., Aly, A., Escandell, J.M., Pieterse, M., Bartkova, J., van der Gulden, H., Hiddingh, S., Thanasoula, M., Kulkarni, A., Yang, Q., et al. (2010). 53BP1 loss rescues BRCA1 deficiency and is associated with triple-negative and BRCA-mutated breast cancers. Nat. Struct. Mol. Biol. *17*, 688–695.

Bunting, S.F., Callén, E., Wong, N., Chen, H.T., Polato, F., Gunn, A., Bothmer, A., Feldhahn, N., Fernandez-Capetillo, O., Cao, L., et al. (2010). 53BP1 inhibits homologous recombination in Brca1-deficient cells by blocking resection of DNA breaks. Cell *141*, 243–254.

Chapman, J.R., Barral, P., Vannier, J.B., Borel, V., Steger, M., Tomas-Loba, A., Sartori, A.A., Adams, I.R., Batista, F.D., and Boulton, S.J. (2013). RIF1 is essential for 53BP1-dependent nonhomologous end joining and suppression of DNA double-strand break resection. Mol. Cell *49*, 858–871.

Chu, W.K., and Hickson, I.D. (2009). RecQ helicases: multifunctional genome caretakers. Nat. Rev. Cancer *9*, 644–654.

Davalos, A.R., Kaminker, P., Hansen, R.K., and Campisi, J. (2004). ATR and ATM-dependent movement of BLM helicase during replication stress ensures optimal ATM activation and 53BP1 focus formation. Cell Cycle *3*, 1579–1586.

Davies, S.L., North, P.S., Dart, A., Lakin, N.D., and Hickson, I.D. (2004). Phosphorylation of the Bloom's syndrome helicase and its role in recovery from S-phase arrest. Mol. Cell. Biol. *24*, 1279–1291.

Deriano, L., Stracker, T.H., Baker, A., Petrini, J.H., and Roth, D.B. (2009). Roles for NBS1 in alternative nonhomologous end-joining of V(D)J recombination intermediates. Mol. Cell *34*, 13–25.

Di Virgilio, M., Callen, E., Yamane, A., Zhang, W., Jankovic, M., Gitlin, A.D., Feldhahn, N., Resch, W., Oliveira, T.Y., Chait, B.T., et al. (2013). Rif1 prevents resection of DNA breaks and promotes immunoglobulin class switching. Science *339*, 711–715.

Eid, W., Steger, M., El-Shemerly, M., Ferretti, L.P., Peña-Diaz, J., König, C., Valtorta, E., Sartori, A.A., and Ferrari, S. (2010). DNA end resection by CtIP and exonuclease 1 prevents genomic instability. EMBO Rep. *11*, 962–968.

Escribano-Díaz, C., Orthwein, A., Fradet-Turcotte, A., Xing, M., Young, J.T., Tkáč, J., Cook, M.A., Rosebrock, A.P., Munro, M., Canny, M.D., et al. (2013). A cell cycle-dependent regulatory circuit composed of 53BP1-RIF1 and BRCA1-CtIP controls DNA repair pathway choice. Mol. Cell *49*, 872–883.

Feng, L., Fong, K.W., Wang, J., Wang, W., and Chen, J. (2013). RIF1 counteracts BRCA1-mediated end resection during DNA repair. J. Biol. Chem. *288*, 11135–11143.

Garcia, A.M., Salomon, R.N., Witsell, A., Liepkalns, J., Calder, R.B., Lee, M., Lundell, M., Vijg, J., and McVey, M. (2011). Loss of the bloom syndrome helicase increases DNA ligase 4-independent genome rearrangements and tumorigenesis in aging Drosophila. Genome Biol. *12*, R121.

Gaymes, T.J., North, P.S., Brady, N., Hickson, I.D., Mufti, G.J., and Rassool, F.V. (2002). Increased error-prone non homologous DNA end-joining—a proposed mechanism of chromosomal instability in Bloom's syndrome. Oncogene *21*, 2525–2533.

Goodarzi, A.A., and Lees-Miller, S.P. (2004). Biochemical characterization of the ataxia-telangiectasia mutated (ATM) protein from human cells. DNA Repair (Amst.) *3*, 753–767.

Grabarz, A., Barascu, A., Guirouilh-Barbat, J., and Lopez, B.S. (2012). Initiation of DNA double strand break repair: signaling and single-stranded resection dictate the choice between homologous recombination, non-homologous end-joining and alternative end-joining. Am. J. Cancer Res. *2*, 249–268.

Gravel, S., Chapman, J.R., Magill, C., and Jackson, S.P. (2008). DNA helicases Sgs1 and BLM promote DNA double-strand break resection. Genes Dev. *22*, 2767–2772.

Guirouilh-Barbat, J., Rass, E., Plo, I., Bertrand, P., and Lopez, B.S. (2007). Defects in XRCC4 and KU80 differentially affect the joining of distal nonhomologous ends. Proc. Natl. Acad. Sci. USA *104*, 20902–20907.

Guirouilh-Barbat, J., Huck, S., Bertrand, P., Pirzio, L., Desmaze, C., Sabatier, L., and Lopez, B.S. (2004). Impact of the KU80 pathway on NHEJ-induced genome rearrangements in mammalian cells. Mol. Cell *14*, 611–623.

Liang, F., Han, M., Romanienko, P.J., and Jasin, M. (1998). Homology-directed repair is a major double-strand break repair pathway in mammalian cells. Proc. Natl. Acad. Sci. USA *95*, 5172–5177.

Nimonkar, A.V., Genschel, J., Kinoshita, E., Polaczek, P., Campbell, J.L., Wyman, C., Modrich, P., and Kowalczykowski, S.C. (2011). BLM-DNA2-RPA-MRN and EXO1-BLM-RPA-MRN constitute two DNA end resection machineries for human DNA break repair. Genes Dev. *25*, 350–362.

Perry, P., and Wolff, S. (1974). New Giemsa method for the differential staining of sister chromatids. Nature *251*, 156–158.

Rass, E., Grabarz, A., Plo, I., Gautier, J., Bertrand, P., and Lopez, B.S. (2009). Role of Mre11 in chromosomal nonhomologous end joining in mammalian cells. Nat. Struct. Mol. Biol. *16*, 819–824.

Sartori, A.A., Lukas, C., Coates, J., Mistrik, M., Fu, S., Bartek, J., Baer, R., Lukas, J., and Jackson, S.P. (2007). Human CtIP promotes DNA end resection. Nature *450*, 509–514.

Sengupta, S., Robles, A.I., Linke, S.P., Sinogeeva, N.I., Zhang, R., Pedeux, R., Ward, I.M., Celeste, A., Nussenzweig, A., Chen, J., et al. (2004). Functional interaction between BLM helicase and 53BP1 in a Chk1-mediated pathway during S-phase arrest. J. Cell Biol. *166*, 801–813.

Simsek, D., and Jasin, M. (2010). Alternative end-joining is suppressed by the canonical NHEJ component Xrcc4-ligase IV during chromosomal translocation formation. Nat. Struct. Mol. Biol. *17*, 410–416.

Tripathi, V., Kaur, S., and Sengupta, S. (2008). Phosphorylation-dependent interactions of BLM and 53BP1 are required for their anti-recombinogenic roles during homologous recombination. Carcinogenesis *29*, 52–61.

Tripathi, V., Nagarjuna, T., and Sengupta, S. (2007). BLM helicase-dependent and -independent roles of 53BP1 during replication stress-mediated homologous recombination. J. Cell Biol. *178*, 9–14.

Weinstock, D.M., Brunet, E., and Jasin, M. (2007). Formation of NHEJ-derived reciprocal chromosomal translocations does not require Ku70. Nat. Cell Biol. *9*, 978–981.

Xie, A., Kwok, A., and Scully, R. (2009). Role of mammalian Mre11 in classical and alternative nonhomologous end joining. Nat. Struct. Mol. Biol. *16*, 814–818.

Yan, C.T., Boboila, C., Souza, E.K., Franco, S., Hickernell, T.R., Murphy, M., Gumaste, S., Geyer, M., Zarrin, A.A., Manis, J.P., et al. (2007). IgH class switching and translocations use a robust non-classical end-joining pathway. Nature *449*, 478–482.